Mesomorphic and Luminescent Polyacetylenes

Jacky W. Y. Lam, Zhiliang Xie, Yuping Dong, Hoi Sing Kwok[†] and Ben Zhang Tang[*]

Department of Chemistry, Hong Kong University of Science & Technology, Clear Water Bay, Hong Kong, China
[†]Center for Display Research, Hong Kong University of Science & Technology, Clear Water Bay, Hong Kong, China
[*]Fax: 852-2358-1594, e-mail: tangbenz@ust.hk

New liquid-crystalline and light-emitting disubstituted polyacetylenes of $-[(CH_3)C=C(CH_2)_9OCO-Biph-O(CH_2)_6CH_3]_n-$, $-[(C_6H_5)C=C(CH_2)_3O-R]_n-$, and $-[(C_6H_5)C=C(CH_2)_3OCOC_6H_4C\equiv C-R]_n-$ (Biph = 4'-4-biphenyl, R = 1-naphthyl, 2-naphthyl, 9-butyl-2-carbazolyl) are synthesized in high yields by metathesis polymerizations catalyzed by WCl_6–Ph_4Sn. All the polymers are completely soluble in common solvents such as THF, chloroform, and toluene. The polymers enjoy excellent thermal stability, losing little of their weights when heated to a temperature as high as 440 °C. The incorporation of biphenyl mesogenic pendants into poly(2-dodecyne) structure endowed the polymer with smecticity. Upon photoexcitation, the polymers emit strong UV and blue lights with quantum efficiency up to 98%. No significant shifts in the emission spectra are observed when the polymers are cast into thin solid films, suggestive of little involvement of aggregative or excimeric emission. Electroluminescence (EL) devices with configuration of $ITO/polyacetylene:PVK/BCP/Alq_3/LiF/Al$ are constructed, which emit blue light with maximum luminance and efficiency of 1136 cd/m^2 and 0.72%, respectively. The polyacetylene light-emitting diodes enjoy outstanding spectral stability, with the EL spectra experiencing little change with an increase in the applied voltage.
Key words: Disubstituted polyacetylenes, mesomorphism, liquid crystal, luminescence, light-emitting diodes.

1. INTRODUCTION

Liquid crystals are molecular optical materials that are widely used in the modern optical display systems. Development of their macromolecular forms, i.e., liquid crystalline polymers, has been a topic of active research. The frontier of polymer research has now been advanced to the utilization of conjugated macromolecules in the construction of electrooptic devices such as light-emitting diodes (LEDs). Polyacetylene is an archetypal conjugated polymer [1–3], which exhibits high electric conductivity upon doping. There have, however, been few scattered examples in the literature regarding the design and synthesis of mesomorphic and luminescent polyacetylenes. The limitation in the variety of such polyacetylenes is due to three reasons. First, to design the molecular structures of the acetylene monomers, we unavoidably have to use functional groups to link the building blocks of pendant groups, triple bonds, and so forth. The introduction of functional groups, however, makes the polymer synthesis difficult because few catalyst systems for acetylene polymerizations have been known to be functionality tolerant [4]. Second, the backbone of polyacetylene is rather rigid. In the community of liquid crystalline polymer research, rigid backbone is generally regarded as defects that distort the packing arrangements of the mesogenic pendants in the mesophases [5–8]. Elaborate design of their molecular structures is thus required. Finally, polyacetylenes are not promising candidates for light-emitting materials because unsubstituted polyacetylene is practically non-emissive. Although blue and green photoluminescence (PL) has been observed in substituted polyacetylenes, their electroluminescence (EL) performances, however, are poor [9–11].

Our group has been interested in the development of functional polyacetylenes. Through careful design of monomer structures and exploration of new catalysts, we have succeeded in preparing a variety of mono- and disubstituted polyacetylenes with novel optical, electronic, organizational, and biological properties [12–23]. In this paper, we report our work on the development of a group of mesomorphic and luminescent disubstituted polyacetylenes.

2. EXPERIMENTAL

2.1 Materials

Poly(9-vinylcarbazole) (PVK), lithium fluoride (LiF), tris(8-hydroxyquinolinato)aluminum (Alq_3), and 2,9-dimethyl-4,7-diphenyl-1,10 -phenanthroline (BCP) were purchased from Aldrich. 12-{[(4'-Heptyloxy-4-biphenylyl) carbonyl]oxy}-2-dodecyne (1), 5-(2-naphth-oxy)-1-phenyl-1-pentyne (2), 5-[({4-[2-(1-naphthyl)-ethynyl]phenyl}carbonyl)oxy]-1-phenyl-1-pentyne (3), and 5-(9-butyl-2-carbazolyloxy)-1-phenyl-1-pentyne (4) were synthesized according to our published procedures [24–26].

2.2 Instrumentation

NMR spectra of the polymers were recorded on a Bruker ARX 300 spectrometer using chloroform-*d* as solvent and tetramethylsilane (TMS) as internal reference. Molecular weights were estimated by a Waters Associates gel permeation chromatography (GPC) system. THF was used as eluent at a flow rate of 1.0 mL/min. A set of Waters monodisperse polystyrene standards covering a molecular weight of 10^3–10^7 was used for the molecular weight calibration. Thermal stability of the polymers was evaluated on a Perkin-Elmer Thermogravimetric Analysis (TGA) 7 at a heating rate of 20 °C/min under nitrogen. A

Perkin-Elmer differential scanning calorimeter (DSC) 7 was used to measure the phase transition thermograms. An Olympus BX 60 POM equipped with a Linkam TMS 92 Hot stage was used to observe anisotropic optical textures. X-ray diffraction (XRD) patterns were recorded on a Philips PW1830 powder diffractometer with a graphite monochromator using 1.5406 Å Cu Kα wavelength at room temperature (scanning rate: 0.05 °/s, scan range 2–30°). The polymer samples for the XRD measurements were prepared by freezing the molecular arrangements in the liquid crystalline states by liquid nitrogen as previously reported [12]. PL spectra of the polymer solutions and films were recorded on a SLM 8000C spectrofluorometer. EL spectra of the polymer films were obtained on a Kollmorgen Instrument PR650 photospectrometer. The luminescence area was 12.6 mm^2. The current-voltage (I-V) characteristics were measured using a Hewlett-Packard HP4145B Semi-conductor Analyzer.

2.3 PL Quantum Yield Measurement

PL efficiency of the polymers was measured according to literature procedure [27, 28]. Both the polymers and the reference 9,10-diphenyl-anthracene were excited at the same wavelength to avoid possible errors caused by neglecting the difference between excitation light intensities of different wavelengths. The quantum yields for 9,10-diphenylanthracene in cyclohexane and poly(methyl methacrylate) (~1 wt %) were 90 and 83%, respectively [27, 28].

2.4 Fabrication of EL devices

Polyacetylene-based LEDs with configurations of ITO/polyacetylene:PVK/BCP/Alq₃/LiF/Al and ITO/8/BCP/Alq₃/LiF/Al were fabricated by sequential spin-coating toluene solutions of the polymers or their blends. The ratio of the polymer to PVK was fixed at 1:4 by weight [29]. The thickness of the emitting layers was in the range of 22–60 nm. BCP (hole blocking layer; 20 nm), Alq₃ (electron transport layer; 30 nm), LiF (electron injection layer; 0.8 nm], and Al were deposited in turn under vacuum (2 × 10^{-6} Torr).

2.5 Polymerization

All polymerization reactions and manipulations were carried out under nitrogen using an inert-atmosphere glovebox (Vacuum Atmosphere), except for the purification of the polymers, which was done in an open atmosphere.

The polymerizations of **1–4** were carried out in toluene at 60 °C for 24 h, using a mixture of WCl₆ and Ph₄Sn as catalyst (Scheme 1). Detailed experimental procedures can be found in our previous paper [12].

Characterization data: **5**: Grey powdery solid; yield 90.7%. M_w 22600; M_w/M_n 8.9 (GPC; polystyrene calibration). ¹H NMR (300 MHz, CDCl₃), δ (ppm): 7.99 (2H, Ar–H ortho to CO₂), 7.48 (4H, Ar–H meta to CO₂ and OCH₂), 6.88 (2H, Ar–H ortho to OCH₂), 4.25 (2H, ArCO₂CH₂), 3.90 (2H, OCH₂), 1.92 (6H, ArCO₂CH₂C*H₂*, =CCH₂CH₂, and OCH₂C*H₂*), 1.30 [18H, (CH₂)₉], 0.88 (CH₃). ¹³C NMR (75 MHz, CDCl₃), δ (ppm): 166.4 (ArCO₂), 159.3 (aromatic carbon linked with OC₇H₁₅), 144.9 (aromatic carbons para to CO₂),

131.9 (aromatic carbons para to OC₇H₁₅), 129.9 (aromatic carbons ortho to CO₂), 128.4 (aromatic carbons meta to OC₇H₁₅), 1278.1 (aromatic carbon linked with CO₂), 126.2 (aromatic carbons meta to CO₂), 114.7 (aromatic carbons ortho to OC₇H₁₅), 67.9 (OCH₂), 64.9 (ArCO₂CH₂), 31.7, 29.2, 29.0, 28.7, 25.9, 22.5, 14.0. UV (THF, 5.9 × 10^{-5} mol/L), λ_max/ε_max: 295 nm/1.99 × 10^4 mol⁻¹ L cm⁻¹.

Scheme 1
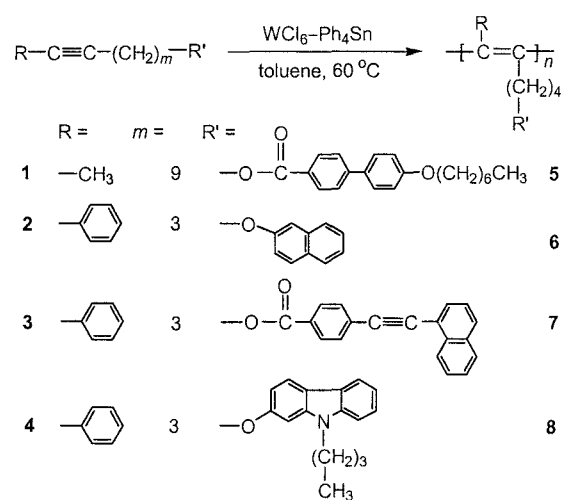
6: Yellow powdery solid; yield 75.1%. M_w 68200; M_w/M_n 1.6 (GPC; polystyrene calibration). ¹H NMR (300 MHz, CDCl₃), δ(ppm): 7.23 (7H, Ar–H), 3.56 (2H, OCH₂), 1.83 (2H, =CCH₂C*H₂*). ¹³C NMR (75 MHz, CDCl₃), δ (ppm): 156.7, 141.4, 134.4, 129.0, 128.6, 127.4, 126.5, 126.1, 123.2, 118.8, 67.9 (OCH₂), 31.0. UV (THF, 3.6 × 10^{-5} mol/L), λ_max/ε_max: 329 nm/0.40 × 10^4 mol⁻¹ L cm⁻¹.

7: Yellow powdery solid; yield 59.0%. M_w 51000; M_w/M_n 2.3 (GPC; polystyrene calibration). IR (KBr), ν (cm⁻¹): 2210 (C≡C). ¹H NMR (300 MHz, CDCl3), δ (ppm): 8.28, 7.68, and 7.51 (1H, Ar–H), 3.86 (2H, CH₂OCO), 1.61 (2H, =CCH₂C*H₂*). ¹³C NMR (75 MHz, CDCl3), δ (ppm): 165.5, 140.5, 133.0, 131.6, 131.3, 131.0, 130.7, 129.4, 128.2, 126.8, 126.4, 126.0, 125.1, 120.2, 93.5 (COC₆H₄C≡), 90.5 (COC₆H₄C≡C), 65.1 (CH₂OCO), 27.5. UV (THF, 2.3 × 10^{-5} mol/L), λ_max/ε_max: 333 nm/2.0 × 10^4 mol⁻¹ L cm⁻¹.

8: Greenish-yellow powdery solid; yield 83.4%. M_w 20500; M_w/M_n 2.0 (GPC; polystyrene calibration). ¹H NMR (300 MHz, CDCl₃), δ (ppm): 7.39–7.21 (7H, Ar–H), 3.56 (4H, OCH₂ and NCH₂Ar), 1.59 (2H, NCH₂C*H₂*), 1.23 [4H, =CCH₂C*H₂* and N(CH₂)₂C*H₂*], 0.80 [3H, N(CH₂)₃C*H₃*]. ¹³C NMR (75 MHz, CDCl₃), δ(ppm): 158.4, 141.5, 140.4, 127.3, 124.0, 123.0, 120.8, 119.3, 118.7, 116.5, 108.3, 107.2, 94.1, 66.7 (OCH₂), 42.5 (NCH₂), 30.5, 20.1, 13.7. UV (THF, 5.3 × 10^{-5} mol/L), λ_max/ε_max: 303 nm/1.73 × 10^4 mol⁻¹ L cm⁻¹.

3. RESULTS AND DISCUSSION

3.1 Monomer and Polymer Syntheses

We designed the molecular structures of a group of acetylene monomers with different mesogenic and chromophoric groups and elaborated multi-step reaction

routes for their syntheses. All the reactions proceeded smoothly and the monomers were obtained in high yields.

Polymerizations of **1**, **2**, and **4** are effected by WCl_6–Ph_4Sn catalyst in toluene at 60 °C, which give high molecular weight polymers (M_w up to 6.8×10^4) in over 50% yield. The same catalyst system can also selectively polymerize the 1-phenyl-1-pentyne structure of **3** without generating any crosslinking products. We characterized the resultant polymers by spectroscopic methods, from which satisfactory analysis data corresponding to their expected molecular structures are obtained.

3.2 Thermal Stability

Notwithstanding the high electrical conductivity of its doped forms, (unsubstituted) polyacetylene has found few, if any, practical applications due to its notorious intractability and instability: the polymer is insoluble in common solvents, infusible before thermal degradation, and degradable upon exposure in air [1–3]. All our polymers are completely soluble in common organic solvents. Are the polymers thermally stable?—This is an important question to be addressed before we study their thermotropic mesomorphism.

Fig. 1 shows the TGA thermograms of the polymers recorded under nitrogen. Polymer **5** does not lose any weight when heated to a temperature as high as 350 °C. The thermal stability of **6–8** is even better with virtually no weight loss being detected when they are heated to 440 °C. The bulky pendant groups may have formed thermally stable "jackets", which wrap up the poly-acetylene backbones and protect them from the attacks of the degradative species [12–14]. The mesogenic and chromophoric pendants contain many aromatic rings, which act as "radical sponges" to trap, deactivate, and/or annihilate the destructive radical species formed in the thermal process [30, 31] and hence enhance the thermal stability of the polymers.
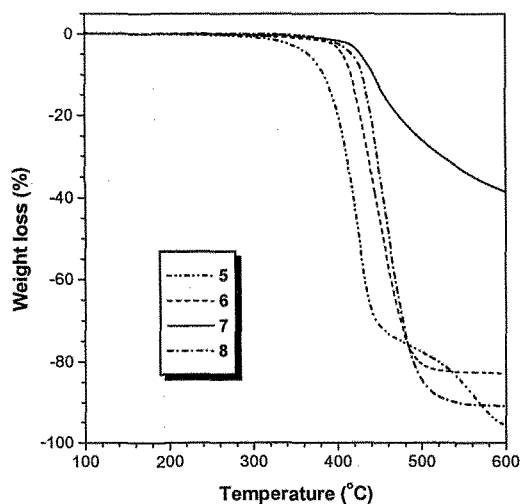

Fig. 1.   TGA thermograms of polyacetylenes **5–8** recorded under nitrogen at a heating rate of 20 °C/min.

3.3 Mesomorphism

To check whether the polymers exhibit liquid crystallinity, we investigated their thermal transitions by

DSC. Polymer **5** enters the S_A phase at 157.3 °C in the 1st cooling cycle (Fig. 2). The mesophase temperature range is wide (~77 °C) and the polymer completely solidifies at 80.0 °C. The 2nd heating cycle shows g–S_A and S_A–i transitions at 99.0 and 163.6 °C, respectively, demonstrating that the mesomorphism of **5** is enantiotropic. We also investigated the thermal properties of **6–8** but none of them displayed liquid crystallinity. It is noteworthy that no irreversible peaks suspiciously associated with polymer degradation are observed at the high temperatures during the cycles of repeated heating–cooling scans. This further proves the high thermal stability of the polymers.
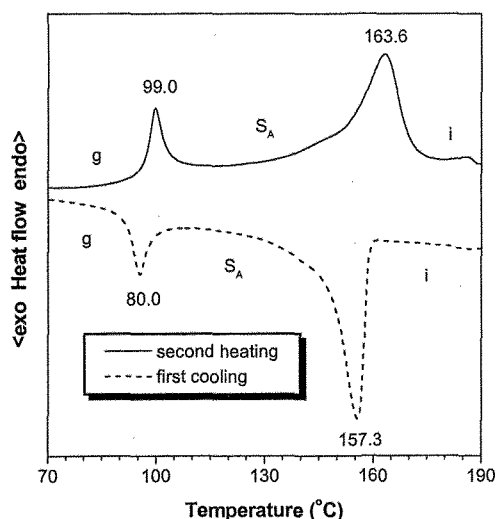

Fig. 2.   DSC thermograms of **5** recorded under nitrogen at a scan rate of 10 °C/min.

Fig. 3 shows the POM micrograph of the mesomorphic texture of **5**. Upon cooling from its isotropic melt, many small bâtonnets emerge. The bâtonnets grow to bigger domains when the sample is further cooled. Further lowering the temperature encourages further growth of the domains and a typical focal conic texture is finally evolved.
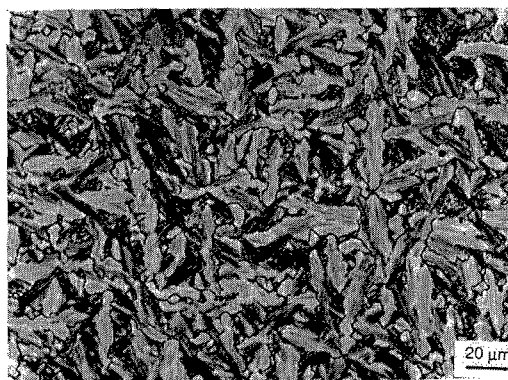

Fig. 3.   Focal conic S_A texture observed on cooling **5** to 135 °C from its isotropic melt.

We carried out X-ray analysis of **5** in order to gain more information on molecular packing arrangements within the mesophase. The diffractogram of **5** displays

a Bragg reflection at a low angle of $2\theta = 2.75°$ and a large peak at a high angle of $2\theta = 20.15°$ (Fig. 4). The *d*-spacing derived from the lowest angle peak is 32.1 Å, which is close to the calculated molecular length for the repeat unit of **5** at its most extended conformation, thus confirming the monolayer S_A nature of the mesophase.
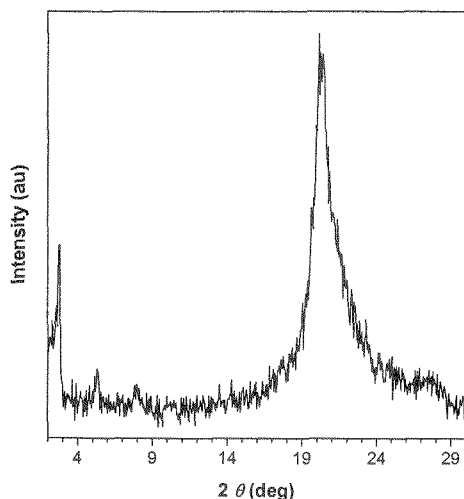

Fig. 4. X-ray diffraction pattern of **5** quenched with liquid nitrogen from its liquid crystalline states at 140 °C.
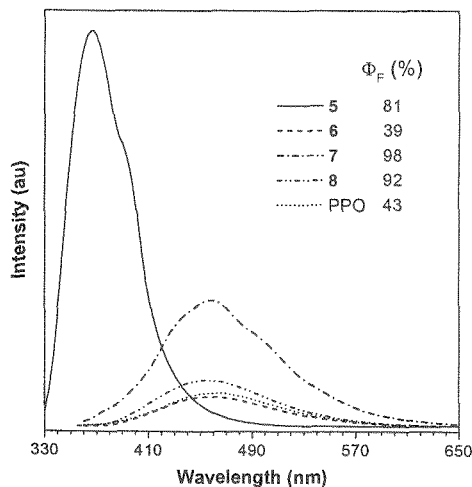

Fig. 5. Photoluminescence spectra of **5–8** and PPO in THF. Concentration: 0.05 mM. Excitation wavelengths (nm): 335 (**5**), 355 (**6** and PPO), 370 (**7**), and 354 (**8**).

3.4 Photoluminescence

We then studied the fluorescence behaviors of our polymers. When a THF solution of **5** is photoexcited at 335 nm, a strong UV light of 369 nm is emitted (Fig. 5). Our previous studies on the luminescence behaviors of mesogen-containing monosubstituted polyacetylenes found that the heptyloxybiphenylcarbonyloxy pendant emitted in the UV region with a λ_{max} of ~369 nm [17]. It thus becomes clear that the emission from the polymer is originated from the pendant chromophores. Using 9,10-diphenylanthracene as reference, the quantum efficiency is calculated to be 81%, which is much higher that of poly(1-phenyl-1-octyne) (PPO), a well-known highly fluorescent disubstituted polyacetylene [5].

Polymer **6**, however, shows very different luminescence behaviors. Upon irradiation at 355 nm, no emission from the naphthalene pendant (~370 nm) is observed. Its PL spectrum is dominated by an emission at 460 nm. Since poly(1-phenyl-1-alkyne)s such as poly(1-phenyl-1-butyne) and PPO emit blue light of 460 nm when excited [17], the emission of **6** at the longer wavelength thus should be stemmed from the poly(pentylalkyne) backbone. The pendant groups in **7** and **8** are more emissive than that in **6**. The emission from the polymers is also found at ~460 nm but with higher efficiency (≥92%), thanks to the efficient energy transfer from the luminophoric pendants to the poly(1-phenyl-1-alkyne) skeleton enabled by the better spectral overlaps between the emission spectra of the pendants and the absorption spectra of the skeletons. This suggests that the optical properties of polyacetylenes are sensitive to their molecular structures and can be easily tuned by incorporation of different chromophoric units into the polymer structures.

Many linear conjugated polymers emit intensely in solution but become weak emitters when fabricated into thin films [32, 33]. This is believed to be caused by aggregate formation: in the solid state, the polymer chains aggregate to form less emissive species such as excimers, leading to a reduction in the luminescence efficiency. Would our polymers suffer the same problem when they fabricated into thin films? Fig. 6 shows the PL spectra of the polymer thin films. Compared to those in solution, no significant shifts in the peak maximums are observed, suggestive of little involvement of aggregate formation. The exact reason for this remains uncertain at the present time. Since PPO also emits in a region similar to that in solution, it seems that the non-aggregative emission is an inherent property for poly(1-phenyl-1-alkyne)s.
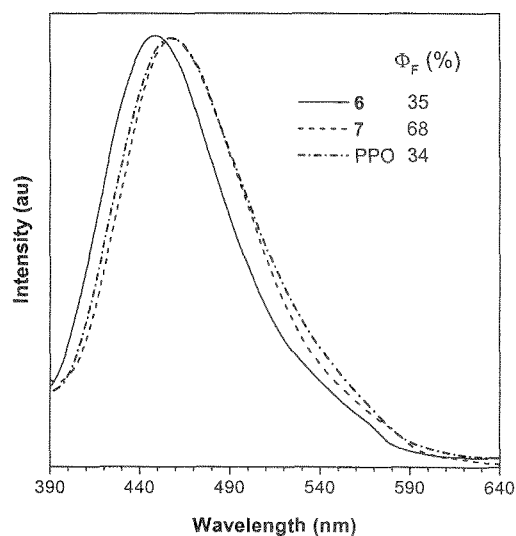

Fig. 6. PL spectra of **6**, **7**, and PPO in solid states. Excitation wavelengths (nm): 355 (**6** and PPO), 370 (**7**).

3.5 Electroluminescence

The efficient PL from our polymers promoted us to study their EL behaviors. A multilayer device with a configuration of ITO/**6**:PVK/BCP/Alq₃/LiF/Al is constructed, using 25% of **6** in PVK as the emitting

layer. The device is turned on at ~8 V, emitting a blue light of 460 nm (Fig. 7). The EL spectrum is single-peaked and symmetrically shaped, with no sidebands associated with such emitting species as excimers. The maximum luminance and external quantum efficiency achieved in the EL device are 511 cd/m^2 and 0.74% at 20 and 12 V, respectively, which are comparable or superior to those of the best blue light-emitting polymers [34, 35]. We also fabricated an EL device of PPO with the same device configuration by replacing **6** with PPO while keeping all other configurational parameters unchanged. No light from the PPO layer is, however, emitted. The comparison data demonstrates that **6** is a better EL material than PPO.
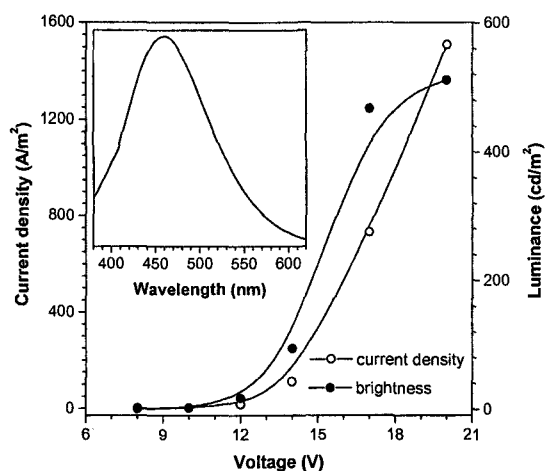

Fig. 7. Changes in the current density and luminance with the applied voltage in a multilayer EL device of **6** with a configuration of ITO/**6**:PVK(1:4 w/w)/BCP/Alq₃/LiF/Al. The inset shows the EL spectrum.

Table I. LED Performances of **6, 7, 8**, and PPO[a]

PA	λ_{max} (nm)	CIE1931 (x, y)	V_{on} (V)	L_{max} (cd/m⁻²)	η_{max} (%)
5	460	0.18, 0.19	8	511	0.74
6	456	0.18, 0.22	11	315	0.21
7	464	0.19, 0.23	13	256	0.17
7[b]	488	0.20, 0.33	8	1136	0.72
PPO[c]	458		14	~1	0.01

[a] Device configuration for all the polymers (unless otherwise specified): ITO/Polymer:PVK(1:4 w/w)/BCP/Alq₃/LiF/Al. Abbreviations: λ_{max} = EL peak maximum, V_{on} = turn-on voltage, L_{max} = maximum luminance, η_{max} = maximum external quantum efficiency. [b] Device configuration: TO/Polymer/BCP/Alq₃/LiF/Al (no PVK used in this device). [c] Device configuration: ITO/PPO/Mg/Al [9-11].

Encouraged by the good result of **6**, we further investigated the device performances of other polymers. Table 1 summarizes the results. All the polymers show a symmetrically shaped EL spectrum with a single peak at ~460 nm. The EL peaks are close to their PL peaks in solution, suggesting that the emissions are truly from the polymers and excimer emissions are unlikely

involved in the EL process. The efficiency of the EL devices varies with the molecular structures of the polymers but all are higher than PPO. It is noteworthy that much better device performance is accomplished in **8** without the aid of PVK, probably due to the hole-transport characteristics of the built-in carbazole rings in the polymer structure. This demonstrates the importance of the device configuration and suggests much room for device configuration improvement.

Among blue light-emitting polymers, poly(fluorene)s have received much attention [36–38]. Their EL devices, however, suffer from such disadvantages as poor spectral stability. The EL spectrum of poly(9,9-dioctylfluorene), for example, broadens with the applied voltage. At 9.2 V, its EL maximum is located at 436 nm, with subpeaks at 463 and 494 nm. When the voltage is increased by 2V to 11.5 V, the 494-nm intensifies, and the EL spectrum broadens and tails into a long-wavelength (>600 nm) region. As a result, the blue emission changes to an undesirable blue-green color. The EL devices of our polymers, however, show much superior spectral stability. The light-emitting diode of **6**, for example, exhibits an EL spectrum with a peak maximum at ~460 nm when a voltage of 10 V is applied (Fig. 8). When the bias voltage is increased to 14 V, The EL spectrum suffers little change. Even when the voltage is raised to 20 V, practically no change is recognizable in the EL spectrum, although the luminance of the device is increased by >250 times.
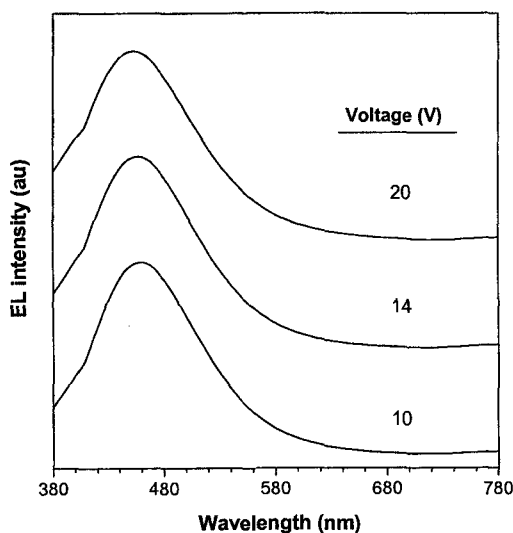

Fig. 8. Stability of the EL spectra of **6** against an applied bias with a device configuration of ITO/**6**:PVK (1:4 w/w)/BCP/Alq₃/LiF/Al.

4. CONCLUSIONS

In this paper, a group of new liquid-crystalline and light-emitting disubstituted polyacetylenes with high molecular weights are prepared in satisfactory yields by acetylene polymerizations initiated by tungsten catalyst. All the polymers are soluble and possess high thermal stability. The incorporation of biphenyl mesogens into the poly(2-dodecyne) structure has endowed the polymer with smecticity. Upon photoexcitation, THF solutions of the polymers emit strong UV and blue lights with quantum efficiency up to 98%. No aggregative or

excimeric emission is observed in the thin solid films of the polymers. Multilayer EL devices utilizing the chromophoric polyacetylenes as emitting layers are constructed, which emit strong blue light with maximum luminance and external quantum efficiency of 1136 cd/m^2 and 0.74%, respectively.

5. ACKNOWLEDGEMENTS

6. REFERENCES

[1] H. Shirakawa, *Angew Chem. Int. Ed.*, **40**, 2575–2580 (2001).

[2] A. G. MacDiarmid, *Angew Chem. Int. Ed.*, **40**, 2581–2590 (2001).

[3] A. J. Heeger, *Angew Chem. Int. Ed.*, **40**, 2591–2611 (2001).

[4] T. Masuda and T. Higashimura, *Adv. Polym. Sci.*, **81**, 121–165 (1987).

[5] J. W. Y. Lam, J. Luo, Y. Dong, K. K. L. Cheuk, and B. Z. Tang, *Macromolecules*, **35**, 8288–8299 (2002).

[6] X. Kong, J. W. Y. Lam, and B. Z. Tang, *Macromolecules*, **32**, 1722–1730 (1999).

[7] B. Z. Tang, X. Kong, X. Wan, H. Peng, W. Y. Lam, X. Feng, and H. S. Kwok, *Macromolecules*, **31**, 2419–2432 (1998).

[8] Y. Mi and B. Z. Tang, *Polym. News*, **26**, 170–176 (2001).

[9] R. G. Sun, T. Masuda, and T. Kobayashi, *Synth. Met.*, **91**, 301–303 (1997).

[10] R. Hidayat, M. Hirohata, K. Tada, M. Teraguchi, T. Masuda, and T. Yoshino, *Jpn. J. Appl. Phys.*, **36**, 3740–3743 (1997).

[11] R. G. Sun, T. Masuda, and T. Kobayashi, *Jpn. J. Appl. Phys.*, **35**, 1434–1437 (1996).

[12] J. W. Y. Lam, Y. Dong, K. K. L. Cheuk, J. Luo, Z. Xie, H. S. Kwok, Z. Mo, and B. Z. Tang, *Macromolecules*, **35**, 1229–1240 (2002).

[13] J. W. Y. Lam, X. Kong, Y. Dong, K. K. L. Cheuk, K. Xu, and B. Z. Tang, *Macromolecules*, **33**, 5027–5040 (2000).

[14] X. Kong and B. Z. Tang, *Chem. Mater.*, **10**, 3352–3363 (1998).

[15] J. Chen, Z. Xie, J. W. Y. Lam, C. C. W. Law, and B. Z. Tang, *Macromolecules*, **26**, 1108–1117 (2003).

[16] Z. Xie, J. W. Y. Lam, Y. Dong, C. Qiu, H. S. Kwok, and B. Z. Tang, *Opt. Mater.*, **21**, 231–234 (2002).

[17] Y. M. Huang, J. W. Y. Lam, K. K. L. Cheuk, W. Ge, and B. Z. Tang, *Macromolecules*, **32**, 5976–5978 (1999).

[18] B. Z. Tang, K. K. L. Cheuk, F. Salhi, B. Li, J. W. Y. Lam, J. A. K. Cha, and X. Xiao, *ACS Symp. Ser.*, **812**, 133–148 (2001).

[19] B. Z. Tang, H. Chen, R. Xu, M. Wang, J. W. Y. Lam, and B. Z. Tang, *Chem. Mater.*, **12**, 213–221 (2000).

[20] B. Z. Tang, H. Xu, J. W. Y. Lam, P. P. S. Lee, K.

Xu, Q. Sun, and K. K. L. Cheuk, *Chem. Mater.* **12**, 1446–1455 (2000).

[21] K. K. L. Cheuk, B. Li, and B. Z. Tang, *Curr. Trends Polym. Sci.*, **7**, 41–55 (2002).

[22] B. Z. Tang, *Polym. News*, **26**, 262–272 (2001).

[23] B. Li, K. K. L. Cheuk, L. Ling, J. Chen, X. Xiao, C. Bai, and B. Z. Tang, *Macromolecules*, **36**, 77–85 (2003).

[24] J. W. Y. Lam, C. K. Law, Y. P. Dong, J. N. Wang, W. Ge, and B. Z. Tang, *Opt. Mater.* **21**, 321–324 (2002).

[25] Y. P. Dong, J. W. Y. Lam, J. A. K. Cha, and B. Z. Tang, *Polym. Mater. Sci. Eng.*, **84**, 539–540 (2001).

[26] J. W. Y. Lam, Ph.D. Dissertation, Hong Kong University of Science & Technology (2003).

[27] J. A. Osaheni and S. A. Jenekhe, *J. Am. Chem. Soc.*, **117**, 7389–7398 (1995).

[28] L. Liao and Y. Pang, *Macromolecules*, **34**, 7300–7305 (2001).

[29] Z. L. Xie, J. W. Y. Lam, C. F. Qiu, M. Wong, H. S. Kwok, and B. Z. Tang, *Polym. Mater. Sci. Eng.*, **88**, 286–287 (2003).

[30] N. S. Allen and M. Edge, "Fundamentals of Polymer Degradation and Stabilization, Elsevier, London (1992).

[31] "Mechanisms of Polymer Degradation and Stabilization", Ed. By G. Scott, Elsevier, London (1990).

[32] M. Grell, D. D. C. Dradley, G. Ungar, J. S. Hill, and K. S. Whitehead, *Macromolecules*, **32**, 5810–5817 (1999).

[33] Y. Li, G. Vamvounis, and S. Holdcroft, *Macromolecules*, **35**, 6900–6906 (2002).

[34] L. C. Palilis, D. G. Lidzey, M. Redecker, D. D. C. Bradley, M. Inbasekaran, E. P. Woo, and W. W. Wu, *Synth. Met.*, **121**, 1729–1730 (2001).

[35] X. Z. Jiang, S. Liu, H. Ma, and A. K. Y. Jen, *Appl. Phys. Lett.*, **76**, 1813–1815 (2000).

[36] G. Zheng, W.-Y. Yu, S.-J. Chua, and W. Huang, *Macromolecules*, **35**, 6907–6914 (2002).

[37] U. Scherf, and E. J. W. List, *Adv. Mater.*, **14**, 477–487 (2002).

[38] F.-I. Wu, D. S. Reddy, C.-F. Shu, M. S. Liu, A. K. Y. Jen, *Chem. Mater.*, **15**, 269–274 (2003).